tissue under stress. J Invest Dermatol 2014;134: 1119–27.

Norris DA, Clark RAF, Swigart LM, Huff JC, Weston WL, Howell SE. Fibronectin fragment(s) are chemotactic for human peripheral blood monocytes. J Immunol 1982;129:1612–8.

Pankov R, Yamada KM. Fibronectin at a glance. J Cell Sci 2002;115:3861–3.

Payne GA, Li J, Xu X, Jackson P, Qin H, Pollock DM, et al. The matrikine acetylated proline-glycine-proline couples vascular inflammation and acute cardiac rejection. Sci Rep 2017;7:7563.

Singer II, Kawka DW, Kazazis DM, Clark RA. In vivo co-distribution of fibronectin and actin fibers in granulation tissue: immunofluorescence and electron microscope studies of the fibronexus at the myofibroblast surface. J Cell Biol 1984;98:2091–106.

Tester AM, Cox JH, Connor AR, Starr AE, Dean RA, Puente XS, et al. LPS responsiveness and neutrophil chemotaxis in vivo require PMN MMP-8 activity. PLoS One 2007;2(3):e312.

Wells A, Nuschke A, Yates CC. Skin tissue repair: matrix microenvironmental influences. Matrix Biol 2016;49:25–36.

Yamada KM, Clark RAF. Provisional matrix. In: Clark RAF, editor. Molecular and cellular biology of wound repair. 2nd ed. New York: Plenum Press; 1996. p. 51–93.

Yi M, Ruoslahti E. A fibronectin fragment inhibits tumor growth, angiogenesis, and metastasis. Proc Natl Acad Sci USA 2001;98: 620–4.

Zhu J, Lin F, Brown DA, Clark RAF. A fibronectin peptide redirects PDGF-BB/PDGFR complexes to macropinocytosis-like internalization and augments PDGF-BB survival signals. J Invest Dermatol 2014;134:921–9.

Intradermal Injection of Bone Marrow Mesenchymal Stromal Cells Corrects Recessive Dystrophic Epidermolysis Bullosa in a Xenograft Model

Journal of Investigative Dermatology (2018) **138,** 2483–2486; doi: 10.1016/j.jid.2018.04.028

TO THE EDITOR

Recessive dystrophic epidermolysis bullosa (RDEB) is caused by loss-of-function mutations in *COL7A1* encoding type VII collagen (C7) that forms anchoring fibrils (AFs), structures essential for dermal-epidermal adherence (Uitto et al., 2017). Patients with RDEB suffer from skin and mucosal blistering and develop severe complications including invasive squamous cell carcinoma, resulting in a poor prognosis (Guerra et al., 2017). Different therapeutic strategies have been explored, including gene-, protein-, cell-based, and pharmacological therapies that have shown promising preclinical or transitory clinical benefits (Rashidghamat and McGrath, 2017). To date, there is no specific treatment for RDEB.

Bone marrow–mesenchymal stromal cells (BM-MSCs) have shown therapeutic potential for RDEB patients through BM transplantation and intradermal (ID) and intravenous injections (Conget et al., 2010; El-Darouti et al., 2016; Petrof et al., 2015; Tamai et al., 2011; Tolar et al., 2009; Wagner et al., 2010). Human bone marrow–mesenchymal stromal cells (hBM-MSCs) form a heterogeneous cell population that can self-renew or differentiate into mesenchymal lineages (Caplan, 1991). hBM-MSCs display properties that could potentially improve wound healing in RDEB: immunomodulation; anti-inflammatory, angiogenic, and antifibrotic properties; secretion of trophic factors; improvement of tissue repair; and the capacity to induce protein expression in the host tissues through a paracrine effect (Nuschke, 2014; Qi et al., 2014).

Herein, we assessed the long-term capacity of hBM-MSCs to survive, produce, and deposit C7 at the dermal-epidermal junction (DEJ) after ID injection into human RDEB skin equivalents (SEs) transplanted onto immune-deficient nude mice that reproduce the skin defect observed in RDEB (Titeux et al., 2010).

Phenotypic analyses of hBM-MSCs from healthy donors showed that they were positive for well-established surface markers (CD105, CD90, CD73, CD29, and CD44) and negative for potential hematopoietic contaminants (HLA-DR and CD45) (see Supplementary Figure S1 online). The capacity of these hBM-MSCs to differentiate in vitro into osteoblasts, adipocytes, and chondrocytes was previously shown (Peltzer et al., 2015).

Then, we compared *COL7A1* expression in hBM-MSCs from several donors cultured with 5% human platelet lysate or 10% fetal calf serum (see Supplementary Figure S2a and b online). C7 expression by hBM-MSCs from donor 1 was similar to human healthy fibroblasts when grown in human platelet lysate, whereas hBM-MSCs from other donors showed lower amounts of C7 (see Supplementary Figure S2c, d, and e).

We next tested the capacity of hBM-MSCs to synthesize C7 able to form AF structures in vivo in a xenograft model. We ID injected hBM-MSCs beneath RDEB SE completely devoid of C7 expression (see Supplementary Figure S3 online), thus excluding any possible paracrine effect of hBM-MSCs on hRDEB fibroblasts and/or keratinocytes, leading to increased production of endogenous mutant C7. The dose of 2×10^6 of hBM-MSC was chosen based on a previous preclinical study (Kuhl et al., 2015). We collected SE samples from the injected area at 1, 2, 4, and 6 months after treatment. Immunofluorescence staining of SE sections showed linear staining of human C7 (see Supplementary Figure S4 online) along the DEJ up to 6 months in healthy SEs and in hBM-MSC–injected RDEB SEs, whereas vehicle-injected RDEB SEs

Abbreviations: AF, anchoring fibril; BM, bone marrow; C7, type VII collagen; DEJ, dermal-epidermal junction; hBM-MSC, human bone marrow mesenchymal stromal cell; ID, intradermal; RDEB, recessive dystrophic epidermolysis bullosa; SE, skin equivalent

Accepted manuscript published online 11 May 2018; corrected proof published online 12 July 2018

© 2018 The Authors. Published by Elsevier, Inc. on behalf of the Society for Investigative Dermatology.

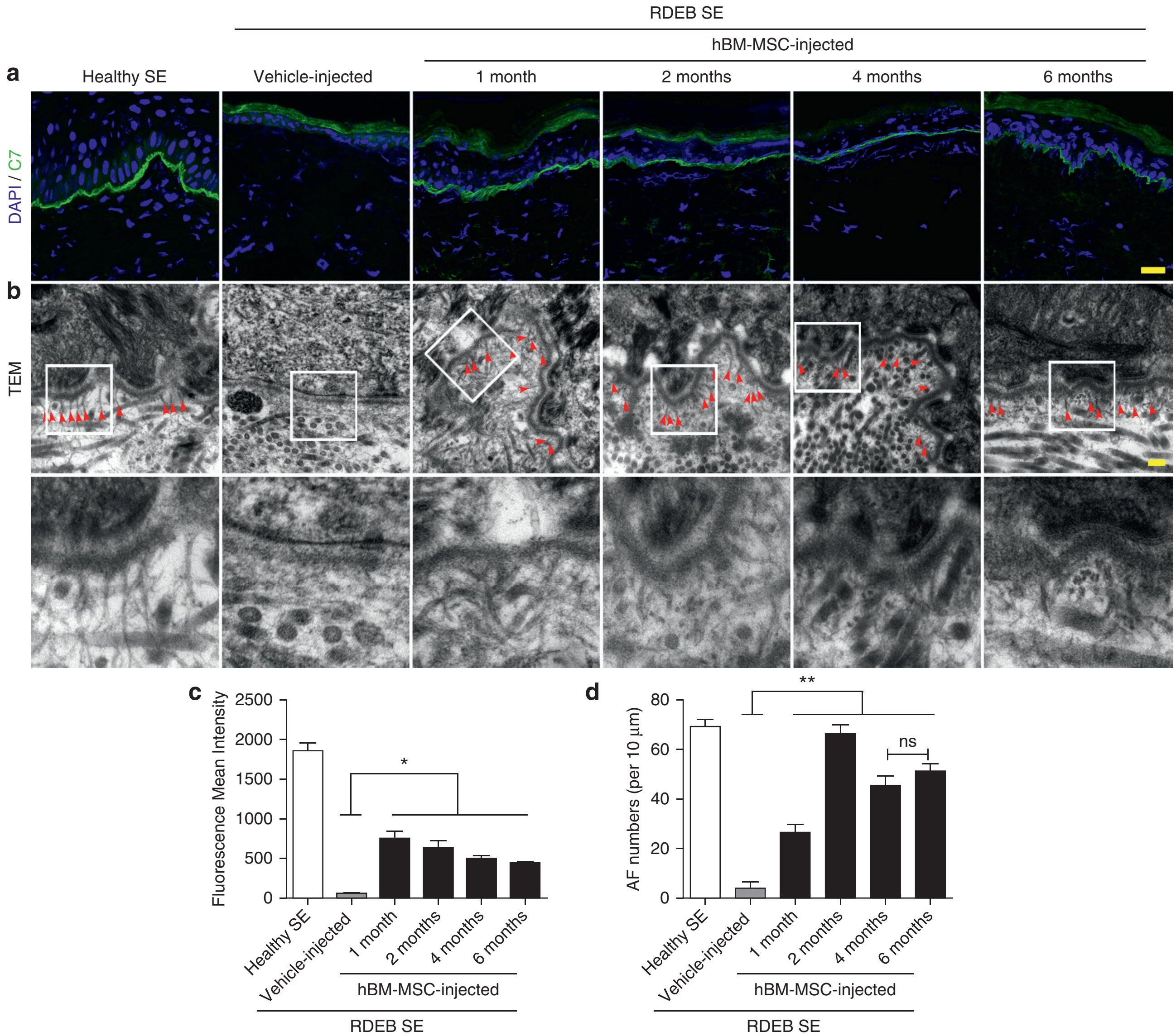

Figure 1. In vivo rescue of C7 expression and AF formation in RDEB SEs injected with hBM-MSCs. (**a**) Immunofluorescence staining of human C7 in noninjected healthy SEs (6 months after grafting); vehicle-injected RDEB SEs (1 month after injection); and RDEB SEs at 1, 2, 4, and 6 months after hBM-MSCs ID injection. hBM-MSC–injected RDEB SE showed re-expression of C7 at the dermal-epidermal junction compared with vehicle-injected RDEB SE. Staining of the stratum corneum with the C7 antibody is nonspecific. Nuclei are stained blue by DAPI. Scale bar = 20 µm. (**b**) Ultrastructural analysis of grafted SE by TEM. Pictures display the presence of AF showing typical loop-shaped structures inserted into lamina densa in hBM-MSC–injected RDEB SE up to 6 months. From 2 to 6 months, the lamina densa is continuous, and AFs are structurally similar to healthy SE. AFs are indicated by red arrowheads. Scale bar = 200 nm. (**c**) Mean average of fluorescence intensity of human C7 protein production over 3 × 5-µm areas in each sample ± standard error of the mean. (**d**) Mean average of number of AFs ≥ 4 in areas of 10 µm of the basement membrane in each sample ± standard error of the mean. Nonparametric Mann-Whitney test. *$P < 0.05$, **$P < 0.01$. n ≥ 3 mice for each time point. AF, anchoring fibril; C7, collagen type VII; hBM-MSC, human bone marrow mesenchymal stromal cell; ID, intradermal; ns, not significant; RDEB, recessive dystrophic epidermolysis bullosa; SE, skin equivalent; TEM, transmission electron microscopy.

showed no detectable C7 staining (Figure 1a). Semiquantitative analysis of C7 fluorescence signal showed that hBM-MSC injection induced a significant increase in C7 deposition (up to 30%–40% of the level of healthy control SE) compared with vehicle-injected RDEB SE (Figure 1c), which is considered to be sufficient to prevent loss of dermal-epidermal adhesion (Fritsch et al., 2008). Similar results were observed after injection of hBM-MSCs from donor 5 in RDEB SEs (see Supplementary Figure S5 online).

Transmission electron microscopy showed the presence of AFs up to 6 months with typical loop-shaped structures inserted into the lamina densa in ID hBM-MSC–injected RDEB SEs and in healthy SEs, but no AF structures were found in vehicle-injected RDEB SEs (Figure 1b). Morphometric analyses showed a significant increase of AF number, especially at 2 months, a time when AF density was similar to healthy SE (95% of healthy control) (Figure 1d, and see Supplementary Figure S6 online).

The fate of injected hBM-MSCs in the RDEB SEs was assessed by fluorescent in situ hybridization using probes specific for human X and Y chromosomes (see Supplementary Figure S7 online), because RDEB SEs were made from human female cells and were injected with hBM-MSCs arising from a

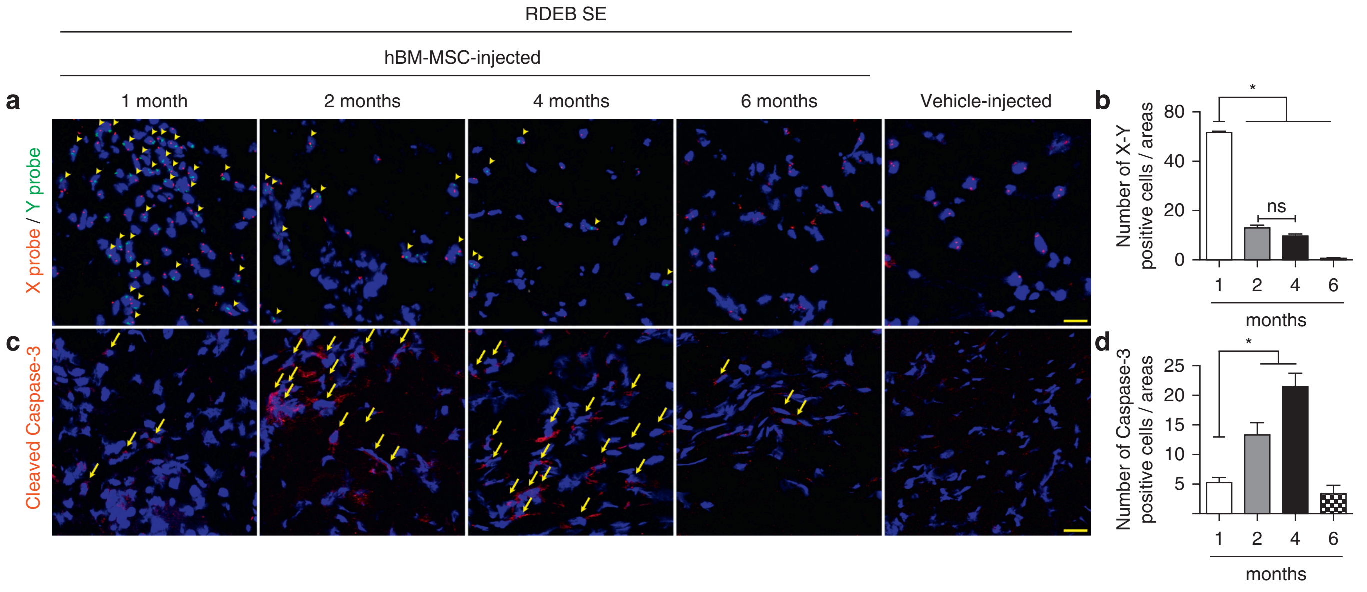

Figure 2. Injected hBM-MSCs are detectable until 4 months in RDEB human SEs. (**a**) FISH analysis of female RDEB SEs at 1, 2, 4, and 6 months after injection of male healthy donor hBM-MSCs, and 1 month after vehicle injection. Because nude mice do not reject human cells, we could follow hBM-MSCs maintenance over time after a single ID injection. Fluorescent X (red) and Y (green) probes in situ hybridization showed detectable X and Y chromosome-positive hBM-MSCs (yellow arrowheads) in the dermis. Nuclei were DAPI stained and considered positive if they contained two nuclear fluorescent spots. The X-probe (red) is the internal positive control. Scale bar = 10 μm. (**b**) Mean average of X and Y chromosome-positive hBM-MSCs over 3 × 5-μm areas in each sample ± standard error of the mean. (**c**) Immunostaining of the active form of caspase-3 was used to detect apoptotic cells in the dermis of RDEB SE injected with hBM-MSCs. Images show nuclei in blue and activated caspase-3 in red for selected time points. Cells positive for active caspase-3 (yellow arrows) show red stain in the cytoplasm. Scale bar = 10 μm. (**d**) Mean average of positive cells for the active form of caspase 3 over 3 × 5-μm areas in each sample ± standard error of the mean. Nonparametric Mann-Whitney test. $*P < 0.05$. $n \geq 3$ mice for each time point. FISH, fluorescent in situ hybridization; hBM-MSC, human bone marrow mesenchymal stromal cell; ID, intradermal; ns, not significant; RDEB, recessive dystrophic epidermolysis bullosa; SE, skin equivalent.

human male donor. Fluorescent in situ hybridization analysis showed the presence of human X-Y chromosome–positive cells in the dermis at 1, 2, and 4 months after injection. No X-Y chromosome–positive cells were found in the dermis of RDEB SE 6 months after injection (Figure 2a). Therefore, injected hBM-MSCs were observed in the dermis of RDEB SEs up to 4 months after injection, but their number clearly diminished over time (Figure 2b). Immunofluorescence staining of the active cleaved caspase-3 showed that hBM-MSC–injected RDEB SEs displayed numerous apoptotic cells in the dermis from 2 to 4 months (Figure 2c), whereas no cells were detected in vehicle-injected RDEB SEs. The number of apoptotic cells expanded up to 4 months and decreased at 6 months, suggesting that most of the injected hBM-MSCs underwent apoptosis between 2 and 4 months after injection (Figure 2d).

Previous RDEB studies using hBM-MSCs showed restoration of C7 at the DEJ for at least 12 weeks, although C7 production decreased over time (Conget et al., 2010; Kuhl et al., 2015). We show a longer effect of hBM-MSCs on C7 production and AF formation (up to 6 months). This is likely due to the extended survival time of injected hBM-MSCs (up to 4 months) compared with the 28 days previously reported (Kuhl et al., 2015), attributable to the lack of immune rejection in our immune-deficient model.

Localized ID injections and the survival of injected hBM-MSCs may represent limitations to treating all symptoms of RDEB. However, ID injections could be repeated over time to sustain clinical benefit in RDEB patients. In addition, systemic delivery of hBM-MSCs could be envisaged, although the extent to which systemic delivery of hBM-MSCs allows engraftment of injected cells in the skin and restoration of C7 is not known (Webber et al., 2017). Therefore, if the treatment has to be repeated for a long period, the risk of allo-reactions to allogeneic hBM-MSCs through the semidirect allorecognition pathway (Alegre et al., 2016) may impair the efficacy of these approaches. An alternative would be to use gene-corrected autologous hBM-MSCs to improve persistence of injected cells and to allow repeated injections.

This study was conducted in accordance with ethical principles stated in the Declaration of Helsinki. Patient consent for experiments was not required, because the French law considers human tissue left over from surgery as discarded material. The mice experiments were performed in compliance with guidelines for animal experiments in France and were approved by the local animal research ethics committee.

CONFLICT OF INTEREST

The authors state no conflict of interest.

ACKNOWLEDGMENTS

This work was supported by grants from the Institut National de la Santé et de la Recherche Médicale (INSERM) and Dystrophic Epidermolysis Bullosa Association (DEBRA) France. The project was granted by a PhD fellowship from the French Ministry of Education, Sciences and Technologies. We thank Araksya Izmiryan, Nathalie Pironon, and Sabine Duchatelet for technical advices. The authors acknowledge Alain Schmitt from Cochin Institute TEM facility for processing skin for transmission electron microscopy analyses and Valérie Malan from the Cytogenetic Department, Necker Hospital for Sick Children, Paris, France. We also acknowledge the Cell Imaging and Animal facilities from Imagine Institute, Paris, France.

Clarisse Ganier[1,2]*, Matthias Titeux*[1,2]*, Sonia Gaucher*[1,2,3]*, Juliette Peltzer*[4]*, Marc Le Lorc'h*[5]*, Jean-Jacques Lataillade*[4]*, Akemi Ishida-Yamamoto*[6] *and Alain Hovnanian*[1,2,5,*]

[1]*Laboratory of Genetic Skin Diseases, INSERM UMR 1163 and Imagine Institute of Genetic Diseases, Paris, France;* [2]*Paris Descartes University—Sorbonne Paris Cite, Paris, France;* [3]*Department of General Surgery, Plastic Surgery and Ambulatory Surgery, AP-HP, HUPC, Cochin Hospital, Paris, France;* [4]*Research and Cell Therapy Department, Military Research Institute (IRBA), Clamart, France;* [5]*Department of Genetics, Necker Hospital for Sick Children, Paris, France; and* [6]*Department of Dermatology, Asahikawa Medical University, Asahikawa, Japan*
[*]*Corresponding author e-mail: alain.hovnanian@inserm.fr*

SUPPLEMENTARY MATERIAL

Supplementary material is linked to the online version of the paper at www.jidonline.org, and at https://doi.org/10.1016/j.jid.2018.04.028.

REFERENCES

Alegre ML, Lakkis FG, Morelli AE. Antigen presentation in transplantation. Trends Immunol 2016;37:831—43.

Caplan AI. Mesenchymal stem cells. Orthop Res 1991;9:641—50.

Conget P, Rodriguez F, Kramer S, Allers C, Simon V, Palisson F, et al. Replenishment of type VII collagen and re-epithelialization of chronically ulcerated skin after intradermal administration of allogeneic mesenchymal stromal cells in two patients with recessive dystrophic epidermolysis bullosa. Cytotherapy 2010;12:429—31.

El-Darouti M, Fawzy M, Amin I, Abdel Hay R, Hegazy R, Gabr H, et al. Treatment of dystrophic epidermolysis bullosa with bone marrow non-hematopoeitic stem cells: a randomized controlled trial. Dermatol Ther 2016;29:96—100.

Fritsch A, Loeckermann S, Kern JS, Braun A, Bosl MR, Bley TA, et al. A hypomorphic mouse model of dystrophic epidermolysis bullosa reveals mechanisms of disease and response to fibroblast therapy. J Clin Invest 2008;118:1669—79.

Guerra L, Odorisio T, Zambruno G, Castiglia D. Stromal microenvironment in type VII collagen-deficient skin: the ground for squamous cell carcinoma development. Matrix Biol 2017;63:1—10.

Kuhl T, Mezger M, Hausser I, Handgretinger R, Bruckner-Tuderman L, Nystrom A. High local concentrations of intradermal MSCs restore skin integrity and facilitate wound healing in dystrophic epidermolysis bullosa. Mol Ther 2015;23:1368—79.

Nuschke A. Activity of mesenchymal stem cells in therapies for chronic skin wound healing. Organogenesis 2014;10:29—37.

Peltzer J, Montespan F, Thepenier C, Boutin L, Uzan G, Rouas-Freiss N, et al. Heterogeneous functions of perinatal mesenchymal stromal cells require a preselection before their banking for clinical use. Stem Cells Dev 2015;24:329—44.

Petrof G, Lwin SM, Martinez-Queipo M, Abdul-Wahab A, Tso S, Mellerio JE, et al. Potential of systemic allogeneic mesenchymal stromal cell therapy for children with recessive dystrophic epidermolysis bullosa. J Invest Dermatol 2015;135:2319—21.

Qi Y, Jiang D, Sindrilaru A, Stegemann A, Schatz S, Treiber N, et al. TSG-6 released from intradermally injected mesenchymal stem cells accelerates wound healing and reduces tissue fibrosis in murine full-thickness skin wounds. J Invest Dermatol 2014;134:526—37.

Rashidghamat E, McGrath JA. Novel and emerging therapies in the treatment of recessive dystrophic epidermolysis bullosa. Intractable Rare Dis Res 2017;6:6—20.

Tamai K, Yamazaki T, Chino T, Ishii M, Otsuru S, Kikuchi Y, et al. PDGFRα-positive cells in bone marrow are mobilized by high mobility group box 1 (HMGB1) to regenerate injured epithelia. Proc Natl Acad Sci USA 2011;108:6609—14.

Titeux M, Pendaries V, Zanta-Boussif MA, Decha A, Pironon N, Tonasso L, et al. SIN retroviral vectors expressing COL7A1 under human promoters for ex vivo gene therapy of recessive dystrophic epidermolysis bullosa. Mol Ther 2010;18:1509—18.

Tolar J, Ishida-Yamamoto A, Riddle M, McElmurry RT, Osborn M, Xia L, et al. Amelioration of epidermolysis bullosa by transfer of wild-type bone marrow cells. Blood 2009;113:1167—74.

Uitto J, Has C, Vahidnezhad H, Youssefian L, Bruckner-Tuderman L. Molecular pathology of the basement membrane zone in heritable blistering diseases: the paradigm of epidermolysis bullosa. Matrix Biol 2017;57—58:76—85.

Wagner JE, Ishida-Yamamoto A, McGrath JA, Hordinsky M, Keene DR, Woodley DT, et al. Bone marrow transplantation for recessive dystrophic epidermolysis bullosa. N Engl J Med 2010;363:629—39.

Webber BR, O'Connor KT, McElmurry RT, Durgin EN, Eide CR, Lees CJ, et al. Rapid generation of Col7a1(-/-) mouse model of recessive dystrophic epidermolysis bullosa and partial rescue via immunosuppressive dermal mesenchymal stem cells. Lab Invest 2017;97:1218—24.

Purinergic Molecules in the Epidermis

Journal of Investigative Dermatology (2018) **138,** 2486—2488; doi: 10.1016/j.jid.2018.04.031

TO THE EDITOR

In the epidermis, adenosine triphosphate (ATP) is released from keratinocytes (KCs) by various environmental stimuli via nonlytic mechanisms, cell damage, or acute cell death (Burnstock et al., 2012). Because ATP is a potent inducer of skin inflammation, it has to be promptly hydrolyzed for the skin to achieve homeostasis (Mizumoto et al., 2003). All experiments that use human and murine materials were performed under institutional approval, and written informed consent was obtained from all subjects. Intradermal injection of ATP induced skin inflammation accompanied by significant neutrophil infiltration (see Supplementary Figure S1a and b online) (Takahashi et al., 2013). Five-week-old BALB/c mice were fed a zinc-deficient (ZD) or zinc-adequate (ZA) diet. As we previously showed (Kawamura et al., 2012), ATP release from the skin in response to an irritant (1% *N,N′*-Bis(acryloyl)cystamine) was significantly increased in ZD mice compared with ZA mice (see Supplementary Figure S1c). However, the amount of ATP contained in the epidermis was comparable between ZD and ZA mice (see Supplementary Figure S1d). This suggests that ATP hydrolysis is attenuated in ZD mice. In the epidermis, ENTPD-1 (CD39), which potently hydrolyzes ATP into AMP, is expressed in Langerhans cells (LCs) in both mice and humans but not in KCs (Georgiou et al., 2005; Ho et al., 2013; Mizumoto et al., 2002). CD39-expressing LCs disappeared from the epidermis of ZD mice (Kawamura et al., 2012). Therefore, the major

Abbreviations: ALP, alkaline phosphatase; AMP, adenosine monophosphate; ATP, adenosine triphosphate; KC, keratinocyte; LC, Langerhans cell; mLC, monocyte-derived Langerhans cell; NHEK, normal human epidermal keratinocyte; ZA, zinc adequate; ZD, zinc deficient

Accepted manuscript published online 11 May 2018; corrected proof published online 14 July 2018

© 2018 The Authors. Published by Elsevier, Inc. on behalf of the Society for Investigative Dermatology.